General Disclaimer

One or more of the Following Statements may affect this Document

- This document has been reproduced from the best copy furnished by the organizational source. It is being released in the interest of making available as much information as possible.

- This document may contain data, which exceeds the sheet parameters. It was furnished in this condition by the organizational source and is the best copy available.

- This document may contain tone-on-tone or color graphs, charts and/or pictures, which have been reproduced in black and white.

- This document is paginated as submitted by the original source.

- Portions of this document are not fully legible due to the historical nature of some of the material. However, it is the best reproduction available from the original submission.

LUMIN

INTERIM REPORT

on

Contract NAS8-31746

SPECKLE REFERENCE BEAM HOLOGRAPHIC AND SPECKLE PHOTOGRAPHIC INTERFEROMETRY IN NON-DESTRUCTIVE TEST SYSTEMS

by

Hua-Kuang Liu

Prepared for

National Aeronautics and Space Administration
George C. Marshall Space Flight Center
Marshall Space Flight Center, Alabama 35812

October 1976

LUMIN Report No. 121-76

Lumin, Inc.

P.O. BOX 5620 TUSCALOOSA, ALABAMA 35401

Table of Contents

List of Illustrations

SPECKLE REFERENCE BEAM HOLOGRAPHIC AND SPECKLE PHOTOGRAPHIC INTERFEROMETRY IN NON-DESTRUCTIVE TEST SYSTEMS

Abstract

The newly-developed techniques of speckle beam holographic interferometry and speckle photographic interferometry will be described. In particular, their practical limitations and their applications to the existing holographic non-destructive test system invented at NASA MSFC will be discussed.

I. Introduction

The grainy or speckle phenomenon of laser light is caused by two of the inherent characteristics of the lasers, i.e., the coherence and monochromaticity of the radiation. Recent development has demonstrated that this phenomenon can be applied in a variety of ways to the measurements of minute surface displacement, surface strains or vibrations of an object. Basically there are two techniques, one is called speckle beam holographic interferometry and the other is called the speckle photographic interferometry. The main advantage of the first technique is its capability of the elimination of the stringent vibration isolation requirement in the present holographic nondestructive test (HNDT) system invented at NASA MSFC. The advantage of the second technique is that the resulting photographic data are only sensitive to the in-plane components of the surface variations. The purpose of this report is to discuss the basic principles and practical limitations of these techniques and their potential applications in the existing HNDT system at NASA MSFC. In particular, three new interferometric non-destructive testing systems are presented. All the systems are based on the NASA MSFC's original HNDT system so that the merits of the original system are preserved and, in the mean time, the advantages of the new techniques can be properly added. Experimental procedures are also outlined for the calibration and evaluation of the new systems in such a way that the comparison of the new systems to the original HNDT system can be made.

II. Basic Principles

A. Double-Exposure Speckle Photographic Interferometry

When a diffuse surface is illuminated by a continuous wave laser, the surface appears to be grainy or speckled. The speckle phenomenon was inter-

preted as a result of two of the fundamental characteristics of lasers[1,2], i.e. monochromaticity and coherence. This is because that any point in front of the illuminated surface receives diffusely scattered light similar amplitudes but random phases from all points on the surface. The interference of these scattered coherent radiation fields naturally give rise to the speckle effect.

The basic principle of the speckle phenomenon can be described[3] with the help of Fig. 1. In Fig. 1, S_1 and S_2 represent two diffuse surfaces illuminated by coherent laser light. Let $\vec{F}_1(x,y,z)$ and $\vec{F}_2(x,y,z)$ be the summations of vectors representing light scattered by all the points from S_1 and S_2 respectively which reach the point $Q(x,y,z)$. Let the resultant amplitude and phase of the light at $Q(x,y,z)$ be written as $\bar{F}_3(x,y,z)$, then

$$\vec{F}_3(x,y,z) = \vec{F}_1(x,y,z) + \vec{F}_2(x,y,z). \tag{1}$$

When x, y, and z vary, the amplitude and phase distributions of $\vec{F}_1$, $\vec{F}_2$, and $\vec{F}_3$ vary accordingly. If the phase at every point of $\vec{F}_1$ changes by the same amount δ relative to $\bar{F}_2$, $\bar{F}_3$ will change in a random manner from point to point. In Fig. 1 consider an area A in the xy plane (with z = constant) over which δ changes equally at all points. Let the intensities at any point $Q(x,y)$ due to S_1 and S_2 be I_1 and I_2 where

$$I_1 = |\vec{F}_1(x,y)|^2 \tag{2}$$

and

$$I_2 = |\vec{F}_2(x,y)|^2 . \tag{3}$$

If the phase angle between $\vec{F}_1$ and $\vec{F}$ is θ when $\delta = 0$, then the resultant intensity may be given by

$$I_3(0) = I_1 + I_2 + 2(I_1 I_2)^{1/2} \cos\theta \,. \tag{4}$$

When $\vec{F}_1$ is shifted by δ in phase with respect to $\vec{F}_2$,

$$I_3(\delta) = I_1 + I_2 + 2(I_1 I_2)^{1/2} \cos(\theta + \delta) \tag{5}$$

In case that a photographic plate is placed in the xy plane and assume that one exposure for 1/2-unit time is made at $\delta = 0$, and another for another 1/2-unit time is made at δ, then the total average energy received at $Q(x,y)$ per unit time is

$$I_3(\delta) = 2(I_1 + I_2) + 2(I_1 I_2)^{1/2} [\cos\theta + \cos(\theta + \delta)] \tag{6}$$

If $\delta = 2n\pi$, where $n = 0, 1, 2, 3, \ldots$, then

$$I_3(2n\pi) = 2\,[I_1 + I_2 + 2(I_1 I_2)^{1/2} \cos\theta]. \tag{7}$$

The distribution of energy in the double exposure record will be the same as the distribution for a single speckle pattern. It can be shown that this distribution may be written as[4,5]

$$W_1(I) = \frac{1}{I_0} \exp\left(\frac{I}{I_0}\right), \tag{8}$$

where $W_1(I)dI$ is the probability that a particular speckle has intensity I, and I_0 is a normalizing factor, which represents the average intensity of the pattern.

If, on the other hand, when $\delta = (2n + 1)\pi$ while I_1 and I_2 remaining constant, then from Eq. (6)

$$I_3(2n\pi + \pi) = 2(I_1 + I_2), \tag{9}$$

This result is equivalent to the effect of incoherently combining two independent speckle patterns. The resultant probability density function becomes

$$W_2(I) = 4 \frac{I}{I_0^2} \exp\left(-\frac{2I}{I_0}\right), \tag{10}$$

where $W_2(I)dI$ is the new probability of a speckle having intensity I.

If T(I) denotes the local intensity transmission of a particular photographic emulsion when exposed to an intensity I for unit time, then for the double exposure corresponding to $\delta = 2n\pi$

$$T_1 = \int_0^\infty W_1(I)\, T(I)\, dI, \tag{11}$$

where $I = I_3(2n\pi)$ as given in Eq. (7). When $\delta = (2n + 1)\pi$, the average transmission becomes

$$T_2 = \int_0^\infty W_2(I)\, T(I)\, dI, \tag{12}$$

where I is given by Eq. (9).

The visibility of the speckle fringes due to the differences of T_1 and T_2 as a result of the two exposures may be defined by

$$V = \frac{T_1 - T_2}{T_1 + T_2}, \tag{13}$$

and the average density D of such a fringe pattern may be defined by

$$D = \log_{10}\left(\frac{2}{T_1 + T_2}\right). \tag{14}$$

B. Speckle Reference Beam Holographic Interferometry

The technique of the speckle reference beam holographic interferometry is completely different from that of the speckle photographic interferometry as described in A above. The speckle reference beam hologram is made in a system similar to the HNDT system used in the NASA Space Sciences Laboratory[6-10]. The system simply consists of a coherent light source being divided into two beams. One beam is used as a reference beam and the other as the object beam. The unique feature of the speckle reference beam technique is that the reference beam is focused to a point on a diffuse surface. The back-scattered light is collected at the film plane[11]. The system can be illustrated by Fig. 2.

If the diffuse surface in Fig. 2 is a part of the object or is fixed to the object, then the motion of the object will be compensated by a change in the path-length of the reference beam. Due to the compensation effect, the stringent vibration isolation requirements associated with conventional holography can be greatly reduced or even completely eliminated.

The conditions of obtaining high-quality reconstructed images with a capability of recording large areas of the object can be derived with the help of Fig. 3. Assume the object is going through random motion. The displaced object is shown with displacement components ΔX and ΔZ. The phase change at the focused reference spot is

$$\Delta\delta_0 = \frac{2\pi\Delta Z}{\lambda}(\cos\beta_0 - \tan\alpha_0 \sin\beta_0 + \sec\alpha_0), \qquad (15)$$

where λ is the wavelength of the laser and the angular parameters are indicated in the Figure. The distance between the object and hologram is considered to be much larger than the random surface displacement. The phase change, $\Delta\delta_n$, at a point on the illuminated portion of the object, is

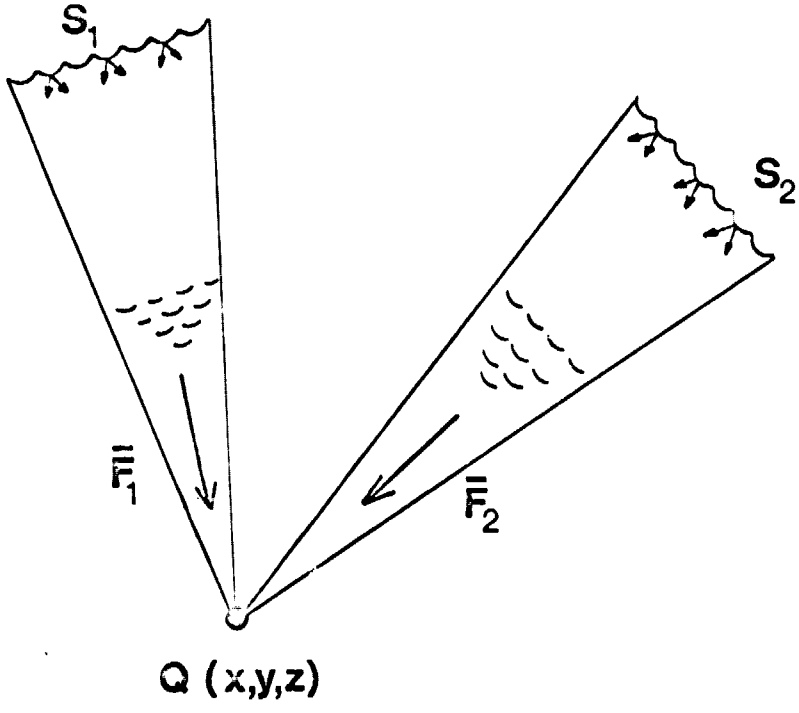

Figure 1. Speckle pattern formation at Q(x,y,z) due to scattering light from S_1 and S_2.

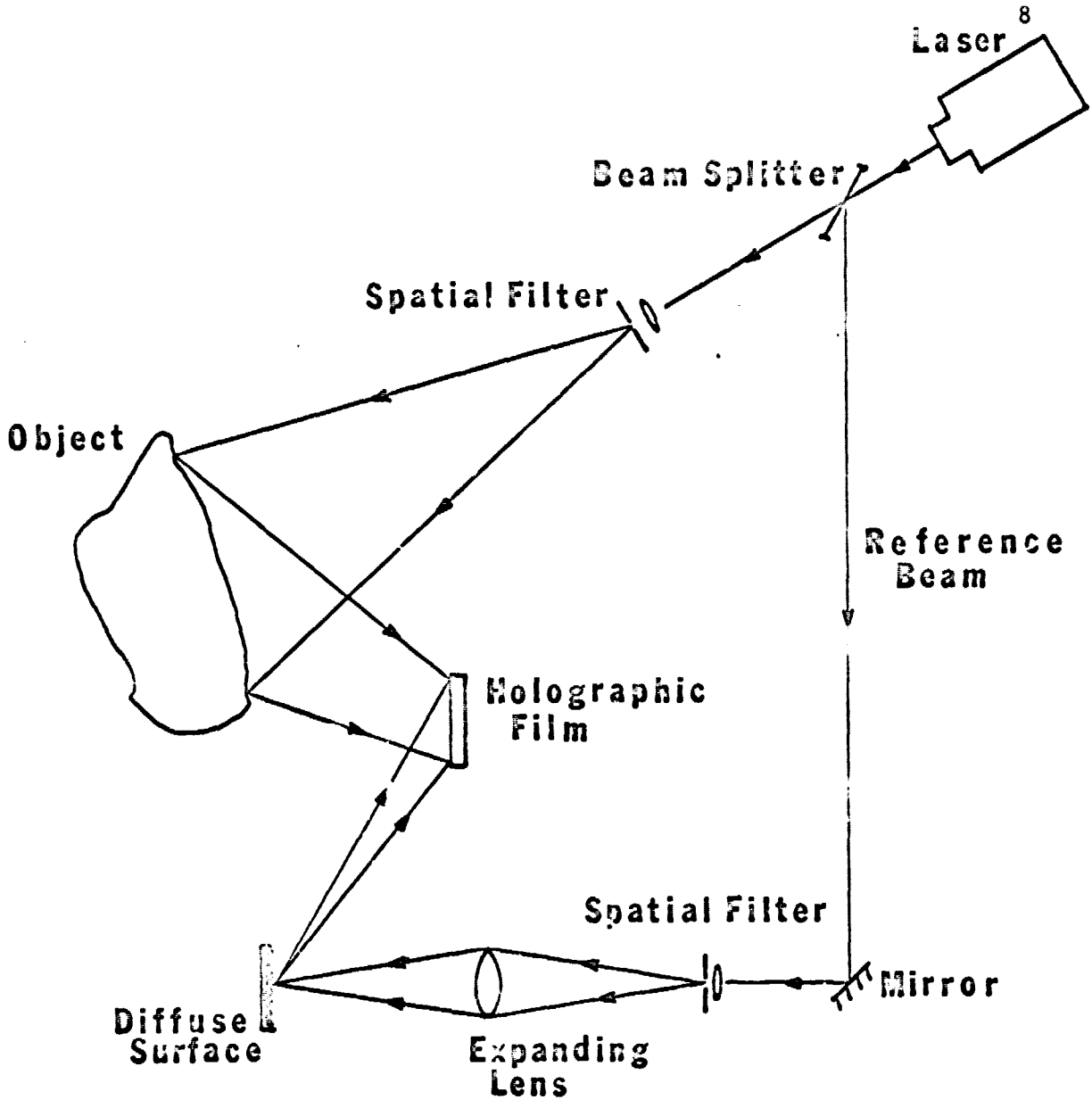

Figure 2. Schematic diagram illustrating a typical speckle reference beam holographic system.

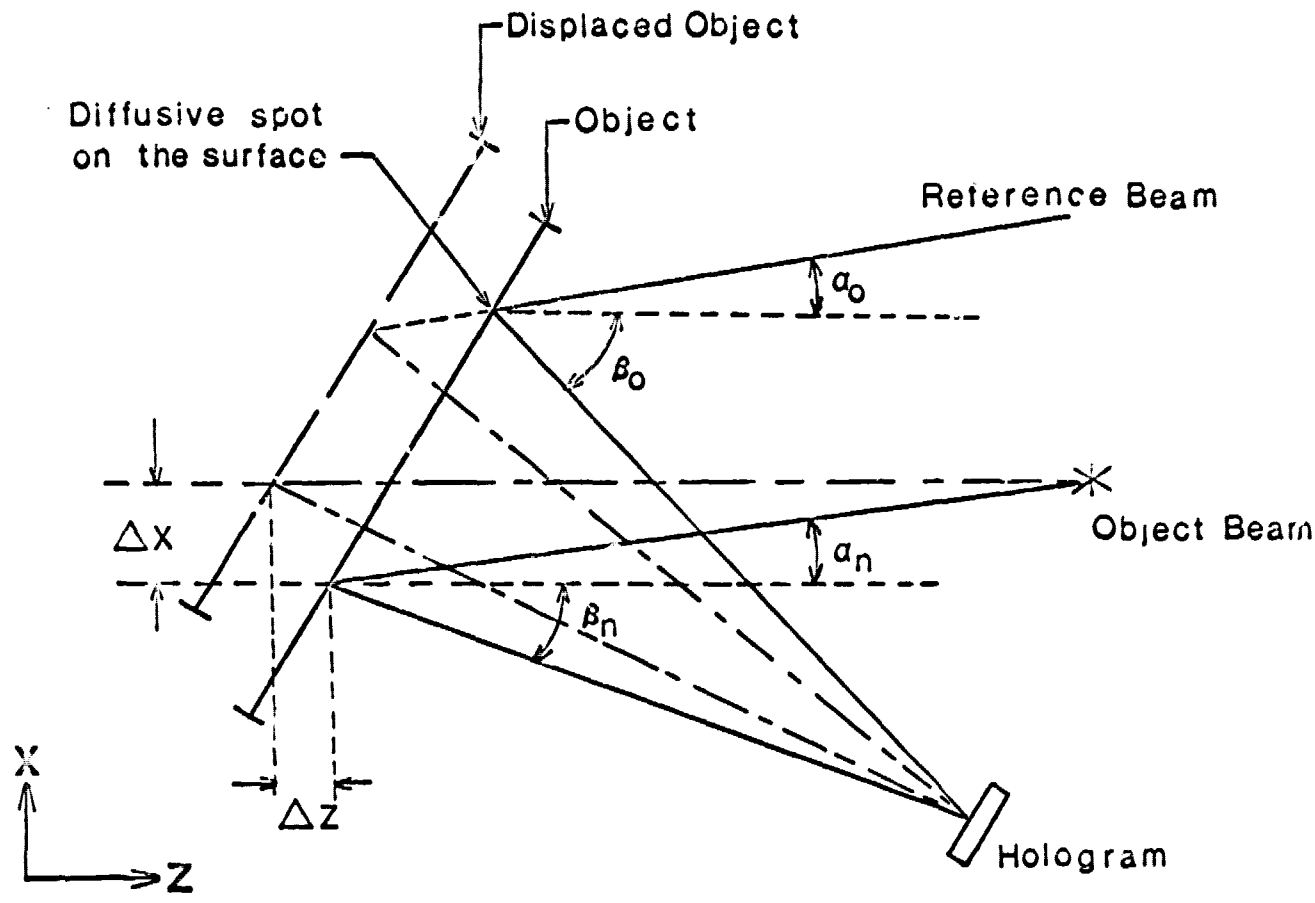

Figure 3. Schematic diagram for the analysis of the speckle reference holographic system.

$$\Delta\delta_n = \frac{2\pi}{\lambda}\left[\Delta Z(\cos\alpha_n + \cos\beta_n) - \Delta X(\sin\alpha_n - \sin\beta_n)\right]. \qquad (16)$$

The validity of the above Equation is based on the assumption that the distance from the illumination point source is much larger than the random displacement of the surface.

Since Eq. (15) is completely independent of ΔX, random motion in the x-direction cannot be compensated. This is a limitation of the present technique. The best one can achieve for random motion compensation in this configuration is to make the two z-components in Eqs. (15) and (16) equal. The conditions are $\alpha_0 = \alpha_n = 0$, and $\beta_n = \beta_0$. Under these conditions maximum object motion compensation is obtained with this technique.

III. Applications of the techniques of Speckle-beam Holographic Interferometry and Speckle Photographic Interferometry in the HNDT System.

The most important advantage of the speckle beam interferometry is that the stringent vibration isolation requirement of the conventional holographic interferometry can be reduced or even eliminated. This is particularly useful for the applications of the holographic nondestructive test systems in realistic testing environment. The important advantage of the speckle photographic intergerometry is its capability of the measurement of the in-plane component of the strain or displacement. Not only one component of the surface changes but also the direction of such a component can be detected. In a previous paper[12], a simple and practical model for the fringe assessment in the HNDT system has been described and the experimental confirmation of the model has been given. It seems that the HNDT system design was already self-contained and quite versatile in its applications to various testing requirements. Nevertheless, it also appears desireable that the advantages of laser speckle patterns can be

utilized so that the capability of the existing HNDT system can even be extended further.

There are many methods that speckle beam holography and speckle photography can be applied to the field of non-destructive testing, however, the following specific goals should be considered in the present applications:

(1) Preserve the present arrangement of the HNDT system as much as possible.

(2) Keep the new arrangement due to the incorporation of the speckle techniques as simple as possible.

(3) Be able to apply or extend the existing theories to the interpretation of the experimental results in the new systems as much as possible.

Based on the above considerations and careful surveys of literature [13-31], three systems are designed. These systems are described in details as follows:

A. Speckle Reference Beam HNDT System

The first new system proposed is shown in Fig.4 . The reference beam is created by the laser light focused on a diffuse spot fixed on the edge of the object. The back-scattered light which consists of speckle patterns distributes over the film plane. The spatial-filter-mirror assembly can be translated so that the anale θ_s can be varied and the sensitivity of the HNDT system can be varied. Several aspects of the system will require experimental studies:

(1) The nature of the diffusive surface, the incidence angle of the laser beam, the size at the focal point of the beam, and the way that the beam was focused should be studied quantitatively.

(2) The reference beam to object beam power ratio and the exposure time need be studied since the speckle patterns are different from the more uniformly expanded reference beams as in the cases of conventional holographic systems.

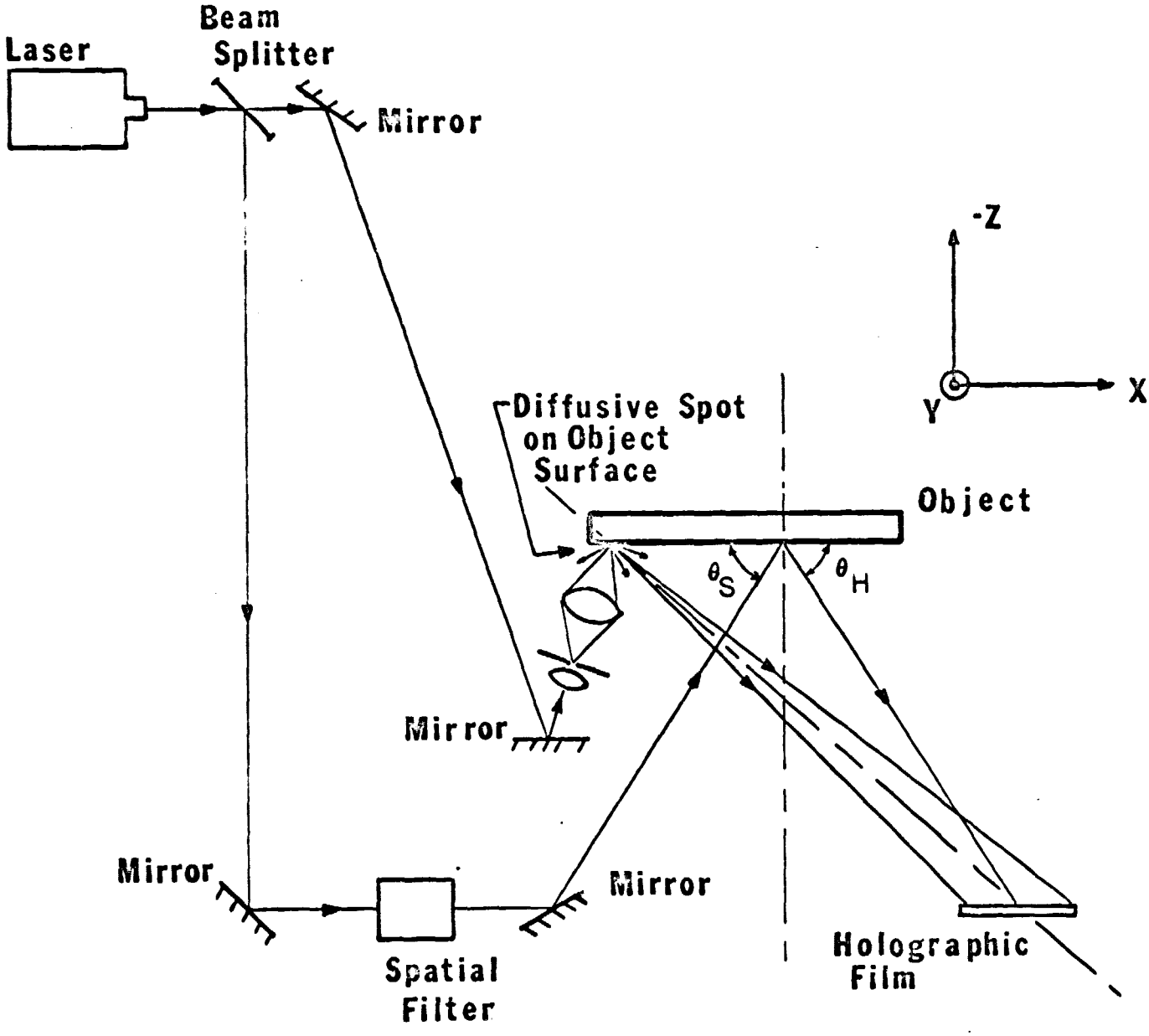

Figure 4. Incorporation of the speckle reference beam in the HNDT system.

(3) Comparison of the speckle beam HNDT system with the existing HNDT system at NASA can be performed by calibrating the system through the flat-plate-translation experiment[12]. The experiment was done on the NASA HNDT system and a practical theoretical model was constructed to explain the results. A comparison between the experimental results of the two system will enable one to see whether the same theoretical model will also be applicable to the speckle beam HNDT system.

B. Symmetrical Speckle-beam Photographic and Holographic Non-destructive Test System.

This new system can best be illustrated by Fig. 5. Two speckle beams are expanded by the spatial-filter-and-mirror assembly enclosed in the boxes of dotted lines. The two beams are illuminating the object from the directions symmetrical with respect to the z-axis. A camera is located along the z-axis in front of the object. In addition, a reference beam which is controlled by shutter B together with a spatial filter and the holographic film can be used to perform the HNDT function. If one of the speckle beam is removed by turning off the light beam by Shutter C, the system becomes identical to the original NASA HNDT system. Hence the result of the present system can be compared with the result of the NASA HNDT system simultaneously in same experiments. This comparison can simply be achieved by alternatively turning on and off the shutters B and C.

The basic principle of the speckle beam photographic interferometry has already been discussed previously. There are several practical considerations worth noting[13]:

(1) Effect of film speed and camera aperture:

The aperture of the imaging lens in the camera is important, because it defines the speckle size and governs the exposure time necessary to record

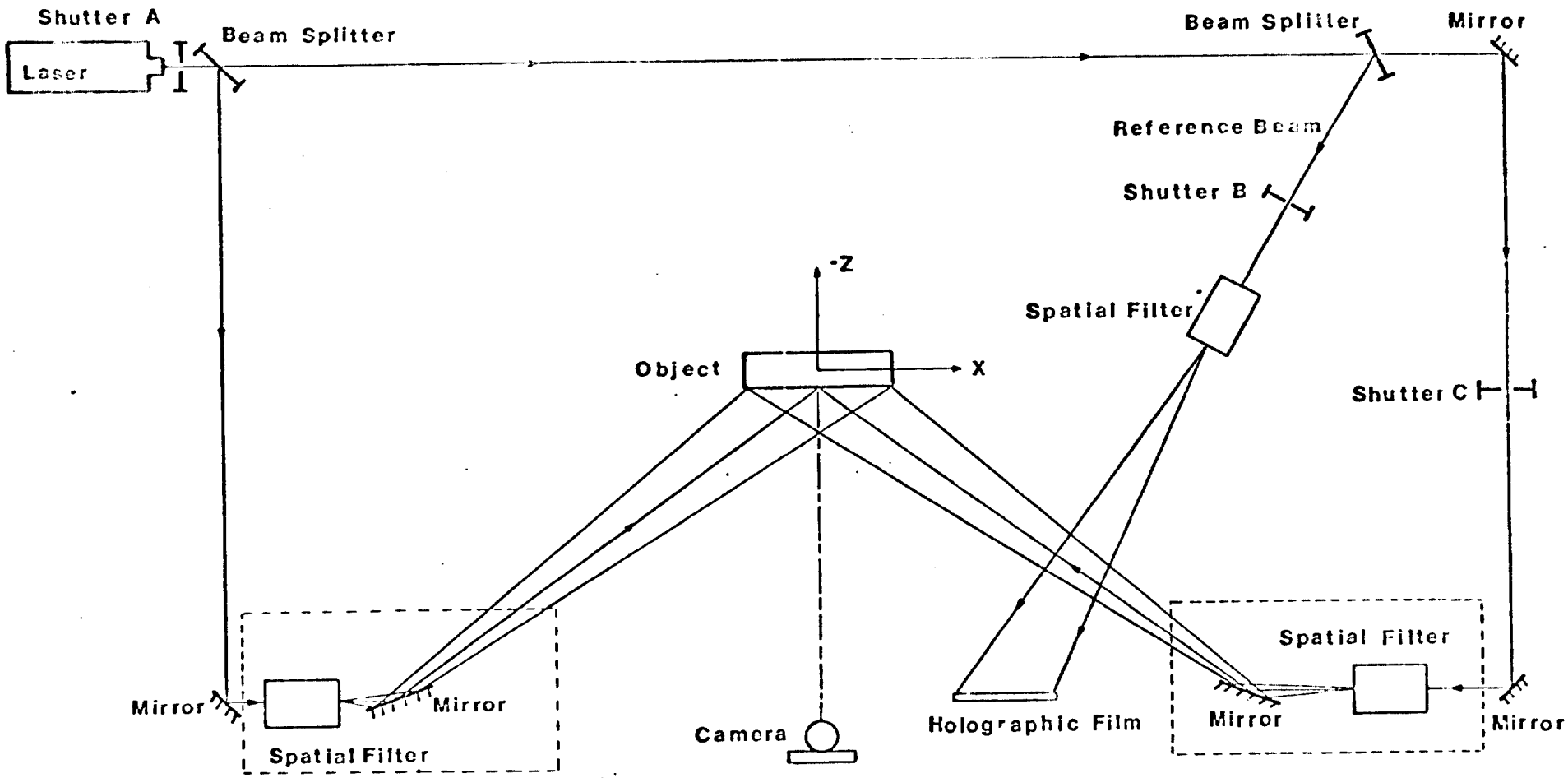

Figure 5. Incorporation of the speckle photographic interferometry with two symmetrical beams in the HNDT system.

the image. If the f number of the aperture is F, the speckle size σ is given approximately by

$$\sigma = 1.2\ \lambda F \tag{17}$$

For the argon laser, the wavelength λ can be chosen at 0.514 μm. At this wavelength, the resolving power of the emulsion must be better than 1600/F lines per mm. It was found that the fine grain Agfa-Gevaert 10E70 film (with a resolution of 2700 lines/mm) can be used as the recording material. A wide range of apertures can be used, and the small dynamic range of the 10E70 allows one to achieve high density with corresponding high fringe visibility for small relative increase in exposure time.

(2) Limitations of the measurable range of object displacement:

It was found that the fringe visibility as defined by Eq. (13) will fall to less than one third of its original value when the lateral displacement ΔX gives rise to an image motion Δx equal to one speckle diameter. The relationship between Δx and ΔX is, $\Delta x = \Delta X/m$, where m is the demagnification factor of the imaging lens.

Since a speckle of size σ on the image corresponds to a speckle of size $m\sigma$ on the object, the number of fringes observable is obtained by equating $m\sigma$ with ΔX in the following equation:

$$2\Delta X \sin\theta = n\lambda, \tag{18}$$

where θ is the angle between the incident speckle beam and the z-axis.

Letting $n = N$, and $\sigma = 1.2\ \lambda F$, the result is the number of fringes observable,

$$N = 2.4\ mF \sin\theta. \tag{19}$$

The number of fringes observable is thus proportional to the demagnification and inversely proportional to the numerical aperture of the lens.

(3) Techniques of extracting the data from the speckled photographs:

Two methods are feasible for the analysis of the data from the speckle photographs[14]. The first method consists of examining the recorded image point-by-point, using a small aperture. An alternative method of analysis is to perform a type of spatial filtering on the film record as illustrated by Fig. 6. The recorded image is first illuminated by a collimated beam of light and then re-imaged by means of a lens. In the focal plane of the lens, a small circular aperture stop is used to select the position of the data from the photograph. If the stop is offset from the axis by azimuth and field angles ϕ and α, the final image is formed only by light diffracted into that direction. Bright areas on the film observed through the aperture will correspond to parts of the object which have gone through a displacement, resolved in the azimuth direction ϕ, of magnitude D^* given by

$$D^* = \frac{n\lambda m}{2 \sin \alpha} , \qquad (19)$$

where n is the order number of the diffraction spectrum. Dark areas correspond to the half-order spectra, where n is replaced by $(n + \frac{1}{2})$ in Eq. (19).

C. Single Speckle-beam Photographic and Holographic Non-destructive Test System.

If only one speckle beam is used, the symmetry of the speckle beams is destroyed, and the system shown in Fig. 5 can be simplified to that shown in Fig. 7. If the lateral surface motion is $d = \sqrt{(\Delta X)^2 + (\Delta Y)^2}$, the corresponding image shift becomes $d = D/m$, where m is the demagnification factor. In this case, the diffraction pattern will consist of a set of Young's fringes having

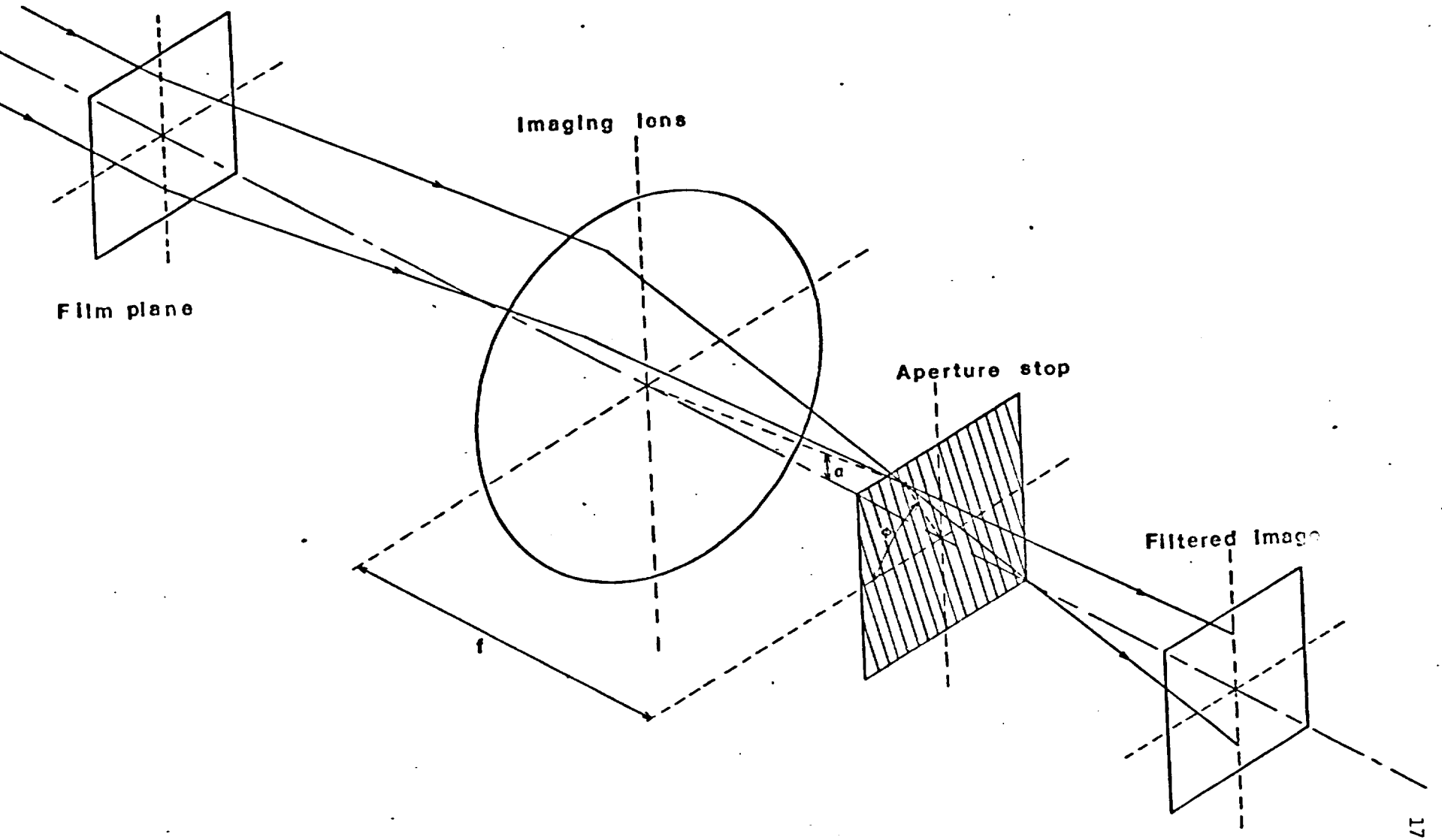

Figure 6. Spatial filtering arrangement for analysis of double-exposure laser photographs.

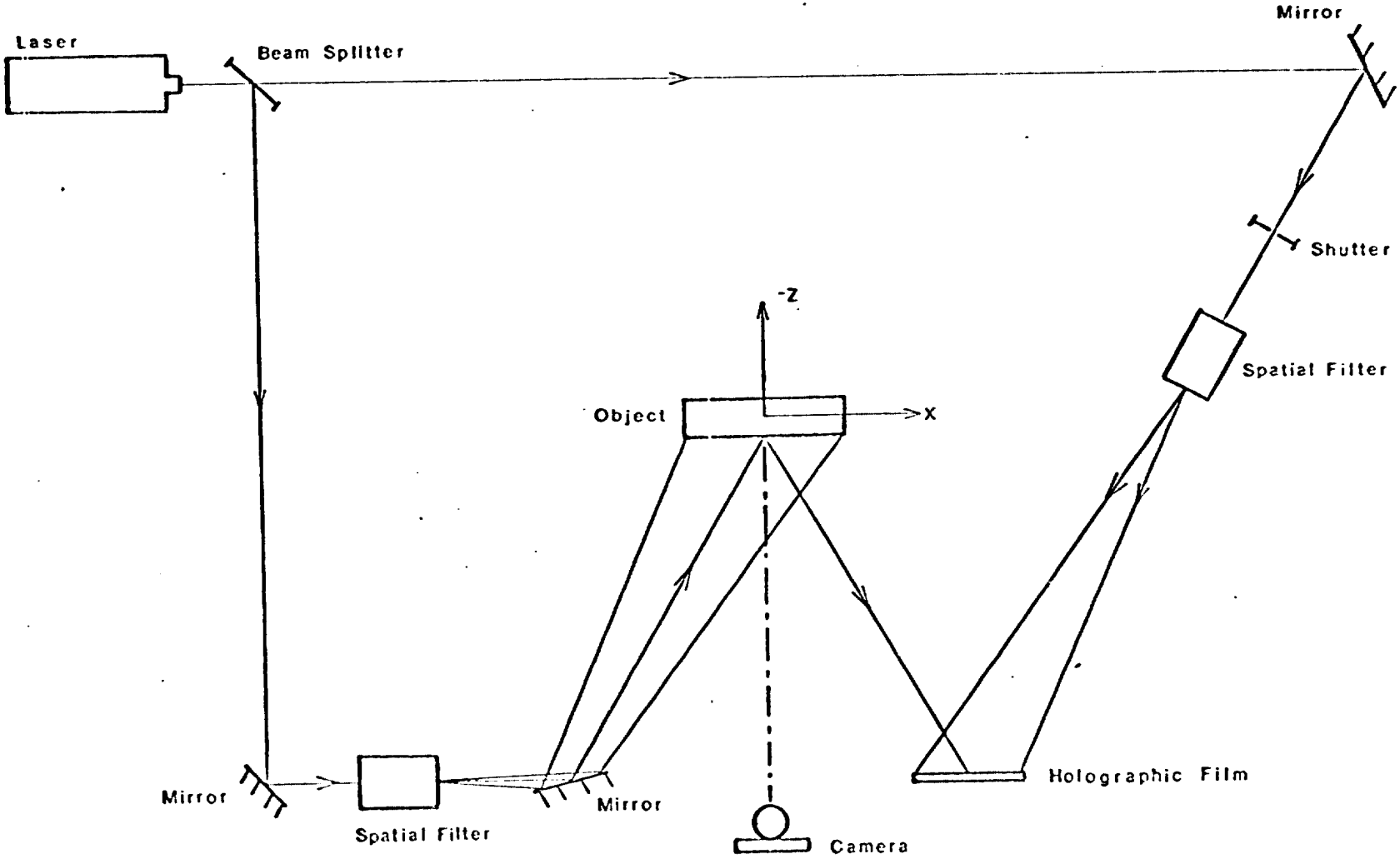

Figure 7. Incorporation of the speckle holographic interferometry with a single speckle beam in the HNDT system.

an angular spacing α given by

$$\sin \alpha = \frac{\lambda m}{d} . \qquad (20)$$

The direction of the fringes will be orthogonal to the direction of the image motion.

The speckle size σ recorded by the film is still the same as that given by Eq. (17). Again, double-exposure holograms can be taken to calibrate the system. The procedures have already been described in the previous sections.

IV. Conclusion

The basic principles of the techniques of speckle-beam holographic interferometry and speckle photographic interferometry have been discussed and the possible ways of incoorperation of these techniques in the existing NASA MSFC's HNDT system have been presented. Three new systems have been depicted with experimental procedures outlined for their evaluations. It is important to note that although the speckle beam inteferometric techniques have many advantages, the fact that they are only sensitive to in-plane motions set a limit to their applications for non-destructive testing especially when the measurements of surface displacements in all directions are required. Hence it seems that it is more appropriate for the speckle techniques to serve auxilary functions in an HNDT system. The new HNDT systems have been proposed on the basis of this principle.

References

1. Allen, L. and Jones, D. G. C., 1963, Phys. Lett. 7, 321-3.
2. Goldfischer, L. I., 1965, J. Opt. Soc. Am. 55, 247-53.
3. Leendertz, J. A., 1970, J. Physics E., 3, 214-218.
4. Lord Rayleigh, 1920, Scientific Papers 6, (Cambridge University Press), pp. 565-610.
5. Goodman, J. W., 1965, Proc. IEEE, 53, 1688.
6. R. L. Kurtz, Appl. Opt., 9, No. 5, May 1970.
7. R. L. Kurtz, NASA TR R-380, January 1972.
8. R. L. Kurtz, U.S. Patent No. 3535014, June, 1972.
9. R. L. Kurtz, and H. K. Liu, NASA TR R-430, June, 1974.
10. H. K. Liu, R. L. Kurtz, NASA TR R-439, May 1975.
11. J. P. Waters, 1972, Appl. Opt. 11, 630-636.
12. H. K. Liu, R. L. Kurtz, 1977, March/April, Optical Engineering.
13. E. Archbold, J. M. Burch and A. E. Ennos, 1970, Optica Acta, 17, 883-898
14. E. Archbold and A. E. Ennos, 1972, Optica Acta, 19, 253-271.
15. J. M. Burch and J. M. J. Tokarski, Opt. Acta 15, 101(1969).
16. E. Archbold, J. Burch, A. Ennos, and D. Taylor, Nature 222, 263(April 1969).
17. R. E. Brooks and L. O. Heflinger, Appl. Opt. 8, 935 (1969).
18. J. Butters and J. Leendertz, J. Phys. E4, 277(1971).
19. B. Eliasson and F. Mottier, J. Opt. Soc. Am. 60, 559 (May 1971).
20. V. Kopf, Optik 33, 517(1971).
21. U. Kopf, Opt. Commun. 5, 346(Aug1 1972).
22. D. Duffy, Appl. Opt. 11, 1728(1972).
23. Y. Hung and J. Der Hovanesian, Exptl. Mech. 12, 454 (Oct. 1972).
24. H. Tiziani, Appl. Opt. 11, 2911(1972).

25. D. Duffy, Exptl. Mech., 14, 378 (Sept. 1974).

26. Y. Hung and C. Taylor, Exptl. Mech., 14, 281(1974).

27. E. B. Aleksandrov and A. M. Bonch-Bruevich, Sov.-Phys. Tech. Phys. 12, 258(1967).

28. K. A. Stetson, J. Opt. Soc. Am., 64, 857-861 (1974).

29. R. Jones and J. A. Leendertz, J. Phys. E., Sci. Inst. 7, 653-657 (1974).

30. Y. Y. Hung, R. E. Rowlands, and I. M. Daniels, Appl. Opt., 14, 618-622 (1975).

31. K. A. Stetson, Opt. Engr., 14, 482-489 (1975).